BRAIN
ORIGINAL ARTICLE

Measures of cortical microstructure are linked to amyloid pathology in Alzheimer's disease

Nicola Spotorno,[1] Olof Strandberg,[1] Geraline Vis,[2] Erik Stomrud,[1,3] Markus Nilsson[2] and Oskar Hansson[1,3]

Markers of downstream events are a key component of clinical trials of disease-modifying therapies for Alzheimer's disease. Morphological metrics like cortical thickness are established measures of atrophy but are not sensitive enough to detect amyloid-beta (Aβ)- related changes that occur before overt atrophy become visible. We aimed to investigate to what extent diffusion MRI can provide sensitive markers of cortical microstructural changes and to test their associations with multiple aspects of the Alzheimer's disease pathological cascade, including both Aβ and tau accumulation, astrocytic activation and cognitive deficits.

We applied the mean apparent diffusion propagator model to diffusion MRI data from 492 cognitively unimpaired elderly and patients with mild cognitive impairment from the Swedish BioFINDER-2 cohort. Participants were stratified in Aβ-negative/tau-negative, Aβ-positive/tau-negative and Aβ-positive/tau-positive based on Aβ- and tau-PET uptake. Cortical regional values of diffusion MRI metrics and cortical thickness were compared across groups. Associations between regional values of diffusion MRI metrics and both Aβ- and tau-PET uptake were also investigated along with the association with plasma level of glial fibrillary acidic protein (GFAP), a marker of astrocyte activation (available in 292 participants).

Mean squared displacement revealed widespread microstructural differences already between Aβ-negative/tau-negative and Aβ-positive/tau-negative participants with a spatial distribution that closely resembled the pattern of Aβ accumulation. In contrast, differences in cortical thickness were clearly more limited. Mean squared displacement was also correlated with both Aβ- and tau-PET uptake even independently from one another and from cortical thickness. Further, the same metric exhibited significantly stronger correlations with PET uptake than cortical thickness ($P < 0.05$). Mean squared displacement was also positively correlated with GFAP with a pattern that resembles Aβ accumulation, and GFAP partially mediated the association between Aβ accumulation and mean squared displacement. Further, impairments in executive functions were significantly more associated with mean squared displacement values extracted from a meta-region of interest encompassing regions accumulating Aβ early in the disease process, than with cortical thickness ($P < 0.05$). Similarly, impairments in memory functions were significantly more associated with mean squared displacement values extracted from a temporal meta-region of interest than with cortical thickness ($P < 0.05$).

Metrics of cortical microstructural alteration derived from diffusion MRI are highly sensitive to multiple aspects of the Alzheimer's disease pathological cascade. Of particular interest is the link with both Aβ-PET and GFAP, suggesting diffusion MRI might reflects microstructural changes related to the astrocytic response to Aβ aggregation. Therefore, metrics of cortical diffusion might be important outcome measures in anti-Aβ treatments clinical trials for detecting drug-induced changes in cortical microstructure.

Received April 12, 2022. Revised August 02, 2022. Accepted August 29, 2022. Advance access publication September 21, 2022

1 Clinical Memory Research Unit, Department of Clinical Sciences, Lund University, Malmö, Lund 223 62, Sweden
2 Diagnostic Radiology, Department of Clinical Sciences, Lund University, 221 85 Lund, Sweden
3 Memory Clinic, Skåne University Hospital, 214 28 Malmö, Sweden

Correspondence to: Nicola Spotorno
Clinical Memory Research Unit
Department of Clinical Sciences
Lund University, Biomedical Research Center, Sölvegatan 17, 223 62, Lund, Sweden
E-mail: nicola.spotorno@med.lu.se

Keywords: cortical diffusion; astrocytes; amyloid-β; Alzheimer's disease

Introduction

Many potential disease-modifying therapies directed against amyloid-beta (Aβ) or tau are currently being developed or evaluated in clinical trials. Markers directly reflecting the biological target (e.g. Aβ or tau) are critical, especially during the early phases to confirm and quantify target engagement. Markers of downstream events, such as neurodegeneration and clinical decline, are also key components in clinical trials, especially during later stages to monitor the response of the participants to the treatment. Clinical and cognitive scores are the most obvious primary outcome measures at this point. However, when targeting upstream pathological events, such as Aβ misfolding and accumulation, therapies will likely be more effective during presymptomatic or prodromal disease stages before overt and irreversible neurodegeneration become more evident.[1,2] In this context, clinical readout might become more challenging and putative makers will be of critical importance.

Recent power calculations comparing structural MRI and promising peripheral markers of neurodegeneration such as plasma level of neurofilament light chain (NfL) have shown that typical MRI metrics, like regional cortical thickness and hippocampal volume, hold some favourable properties as an outcome measure in clinical trials when compared to NfL. MRI provides for clearly lower within-subject variability than NfL, meaning that a relatively small difference in atrophy rate can be detected by such metrics in a longitudinal clinical trial.[3] Metrics derived from structural MRI are routinely used as a proxy of regional neurodegeneration and have already been included as secondary outcomes in several clinical trials for immunotherapies targeting Aβ.[4–7] However, the results from such trials have been puzzling. Therapies that clearly reduced Aβ burden seemed to lead to an increase in atrophy, as quantified by structural MRI.[4,5] As this is unlikely an indication of worsened neurodegeneration, other hypotheses have been put forward. For example, the reduction of Aβ pathology has a significant impact on the neuroinflammatory response, which entails a change in the morphology and distribution of glial cells in the cortex.[8,9] Another related hypothesis involves fluid shifts between intracellular and extracellular or intravascular compartments, which could be detected as a change in volume.[9] These hypotheses suggest that microstructural changes occur as an effect of anti-Aβ therapies and the currently available morphological MRI measures seems to be poorly equipped for monitoring these effects.

Diffusion MRI (dMRI) probes microstructural properties of tissues by investigating the random displacement of water molecules.[10] dMRI has traditionally been used to investigate white matter, but dMRI metrics can also be extracted from the cortex. Previous works showed encouraging results across different neurodegenerative diseases. Studies using diffusion tensor imaging (DTI) proposed that the so-called mean diffusivity is a sensitive marker of an underlying neurodegenerative process. For example, mean diffusivity appeared to be more sensitive to structural changes than cortical thickness in a study on the behavioural variant frontotemporal dementia.[11] In the Alzheimer's disease spectrum mean diffusivity appears to be able to detect differences even in the preclinical stages in both sporadic and genetic cases,[12,13] with some evidence linking increased mean diffusivity to tau accumulation.[14] Studies using biophysical modelling such as the neurite orientation dispersion and density imaging (NODDI) technique[15] have also suggested that metrics derived from dMRI are sensitive to pathological changes during different stages of the Alzheimer's disease continuum.[16–18] However, no dMRI measure has thus far been consistently shown in a large cohort to be associated with Aβ aggregates, independent from insoluble tau aggregates, which is important if such a measure should be used in anti-Aβ trials.

In the present study, we explored the associations between metrics of cortical diffusion, protein aggregation and atrophy focusing on a large cohort of non-demented individuals, including cognitively unimpaired individuals and patients with mild cognitive impairment. Participants were stratified following the AT framework[19] according to previously published Aβ- and tau-PET cut-offs. Specifically, we investigated the differences in regional cortical diffusion between groups as well as the potential association between cortical diffusion and both Aβ- and tau-PET retention across the entire neocortex. We further focused the analysis on meta-regions of interest encompassing the regions that are most reliably associated with Aβ and tau accumulation and we test to what extent cortical diffusion is associated with cognitive performance in domain that has been associated with Aβ pathology (i.e. executive functions[20]) and tau pathology (i.e. memory functions). For all analyses we also tested to what extent the effect of cortical diffusion was independent of overt atrophy, quantified by cortical thickness. We also tested the possible association between cortical diffusion and plasma levels of NfL, another marker of neurodegeneration. Considering that glial activation appears to have a significant role in the pathophysiology of Alzheimer's disease[21–23] and, possibly, in the response to anti-Aβ disease-modifying therapies,[8] we further investigated the association between cortical diffusion and plasma levels of glial fibrillary acidic protein (GFAP), a marker of astrocytic activation, which has been shown to correlate with Aβ-PET retention.[24]

Cortical diffusion was quantified by fitting the mean apparent propagator model (MAP-MRI)[25,26] to the dMRI data. MAP-MRI is a non-parametric framework that efficiently measures the probability

density function (PDF) of spin displacements allowing derivation of useful metrics indicative of diffusion in complex microstructures. MAP-MRI extends the DTI model taking full advantage of modern dMRI sequences and providing metrics that could be more sensitive to subtle pathological events taking place during the first stages of the disease process.[27] Two of the most commonly derived metrics are the mean squared displacement (MSD) and the return to the origin probability (RTOP), which describe different although complementary aspects of water diffusion. More specifically, MSD quantifies the average amount of diffusion, with an increase in MSD indicating that protons are less hindered/restricted. RTOP quantifies the probability that a proton will be at the same position at the first and second diffusion gradient pulse and has been proposed to reflect cellularity, size of cell bodies or presence of restricting barriers (e.g. in the presence of myelin).[27] In contrast to biophysical models, such as NODDI, MAP-MRI makes no assumption on the property of the diffusion in tissues, which could be beneficial especially when testing disease state, where the theoretical assumptions of biophysical models are unlikely to hold.[28,29]

Materials and methods

Participants

Five hundred and forty-three participants from the Swedish BioFINDER-2 study were included. Only participants with available structural and diffusion MRI scans, ^{18}F-flutemetamol PET and ^{18}F-RO948 PET and age > 50 years were included in the study cohort. To capture the entire spectrum of early Alzheimer's Disease development from subthreshold Aβ levels to abnormal Aβ levels and finally cognitive symptoms, cognitively unimpaired participants and patients with mild cognitive impairment (MCI) with evidence of Aβ pathology were included (see Supplementary material for inclusion and exclusion criteria). Quality control procedures on the diffusion scans, based on visual assessment of raw and processed data, blinded to clinical diagnosis, led to the exclusion of 51 scans due to poor data quality. Therefore, 492 participants were included in the final cohort. Participants were stratified in Aβ-negative/tau-negative, Aβ-positive/tau-negative and Aβ-positive/tau-positive based on Aβ- and tau-PET uptake. Demographic and clinical characteristics are summarized in Table 1. All subjects gave written informed consent according to the Declaration of Helsinki, and the study was approved by the Ethical Review Board of Lund, Sweden.

Imaging protocol and analysis

PET protocol

Participants underwent ^{18}F-flutemetamol PET and ^{18}F-RO948 PET on Discovery MI scanners (GE Healthcare). ^{18}F-Flutemetamol PET images were acquired 90–110 min after injection of 185 MBq ^{18}F-flutemetamol while ^{18}F-RO948 PET images were acquired 70–90 min after injection of 370 MBq ^{18}F-RO948. Preprocessing and generation of standardized uptake value ratio (SUVR) maps was carried out as described in previous reports.[30,31] ^{18}F-Flutemetamol scans were normalized using the Pons as reference region, while the inferior cerebellar grey matter was chosen as reference region for ^{18}F-RO948. Aβ status was defined based on Aβ-PET uptake in a neocortical composite region using a previously published cut-off of 0.53,[30] while tau positivity was defined based on tau-PET uptake from a temporal composite region using a previously published cut-off of 1.36.[31]

Table 1 Demographic summary of the study cohort

	Aβ-negative/ tau-negative	Aβ-positive/ tau-negative	Aβ-positive/ tau-positive
n (% female)	271 (55%)	143 (50%)	78 (55%)
Age	66 (10)	71 (8)[a]	73 (8)[a]
Years of education	13 (4)	12 (4)	13 (5)
MMSE	29 (1)	28 (2)	27 (2)[a]
APOE ϵ4 (%)	93 (36%)	92 (66%)[a]	60 (78%)[a]
Trail making —A, s	37 (12)	49 (22)[a]	53 (23)[a]
Trail making —B, s	82 (33)	107 (45)[a]	136 (58)[a]
ADAS delayed recall	3 (2)	4 (2)[a]	7 (2)[a]

Values are given as mean (SD). Aβ positive/negative according to a previously published cut-off of 0.53 based on Aβ-PET uptake in a neocortical meta-region of interest[29]; tau positive/negative based on tau-PET uptake in a temporal meta-region of reflecting Braak stages I–IV, using a previously published cut-off of 1.3.[30] ADAS = Alzheimer's Disease Assessment Scale; MMSE = Mini Mental State Examination.
[a]Significantly different from the Aβ-negative/tau-negative ($P < 0.05$).

MRI protocol

MRI scans were performed on the same MAGNETOM Prisma 3 T scanner (Siemens Healthcare), equipped with a 64-channel head coil. A single-shot echo-planar imaging sequence was used to acquire 104 diffusion-weighted imaging volumes (repetition time: 3500 ms; echo time: 73 ms; resolution: $2 \times 2 \times 2$ mm^3; field of view $220 \times 220 \times 124$ mm^3; b values range: 0, 100, 1000 and 2500 s/mm^2 distributed over 2, 6, 32 and 64 directions; 2-fold parallel acceleration and partial Fourier factor = 7/8). A T_1-weighted MPRAGE (magnetization-prepared rapid gradient-echo) sequence was also acquired with the following acquisition parameters: inversion time: 1100 ms; flip angle: 9 degrees; echo time: 2.54 ms; echo spacing: 7.3 ms; repetition time: 1900 ms; receiver bandwidth: 220 Hz/pixel; voxel size: $1 \times 1 \times 1$ mm^3. GRAPPA (generalized autocalibrating partially parallel acquisitions[32]) was applied with acceleration factor of 2 and 24 reference lines.

MRI processing

Processing of structural data

MPRAGE images were preprocessed using FreeSurfer (version 6.0, https://surfer.nmr.mgh.harvard.edu). FreeSurfer pipeline includes several steps such as correction for intensity homogeneity,[33] removal of non-brain tissue[34] and segmentation into grey and white matter.[35,36] Cortical thickness was estimate as the distance from the grey matter/white matter boundary to the corresponding pial surface.[37] Cortical thickness values were extracted from the 68 cortical regions of the Desikan–Killiany–Tourville atlas included in FreeSurfer.

Processing of diffusion-weighted images

The dMRI data were processed by using a combination of open-source algorithms. The acquired images were corrected for susceptibility-induced distortion using images acquired with opposite phase polarities, motion and Eddy currents employing FSL tools (FMRIB Software Library, version 6.0.4; Oxford, UK). The regularized MAP-MRI model was fitted using the implementation provided by DIPY (v1.4.1) using standard parameters (see https://dipy.org/documentation/1.4.1./examples_built/reconst_mapmri/#example-reconst-mapmri) and voxel-wise maps of the MSD and RTOP[38]

were generated for each participant. Finally, to render the RTOP comparable across subjects, the metric was normalized by the average ventricular RTOP of each subject's, which approximate the RTOP values in free water for each acquisition.[39,40]

Surface projection of RTOP and MSD

The diffusion images (using the average of the b0 volumes) were co-registered to each subject's MPRAGE image using ANTs routines (v2.1) and both MSD and RTOP maps were warped to the same space. MSD and RTOP were then sampled at three equidistant points between white and pial surfaces starting and stopping within 25% from the borders of the cortical ribbon and averaged providing a single MSD or RTOP value for each vertex of the subject's cortical surface. These processing steps were performing using FreeSurfer commands as previously reported by other groups.[13,14] Finally, MSD and RTOP values were extracted from the 68 cortical regions of the Desikan–Killiany–Tourville atlas.

Plasma protocol and analysis

Blood was collected in six EDTA-plasma tubes and centrifuged (2000*g*, +4°C for 10 min). After that, plasma was aliquoted into 1.5-ml polypropylene tubes (1 ml plasma in each tube) and stored at –80°C within 30–60 min of collection. GFAP, a marker of astroglial activation and astrocytosis, was analyaed in 292 participants using Discovery kits for HD-X (Quanterix®). GFAP, a marker of astroglial activation and astrocytosis, was analysed in 292 participants using Simoa immunoassay. In the same group of participants plasma levels of NfL were analysed using the commercially available Simoa immunoassay. The analysis was performed by board-certified laboratory technicians who were blinded to clinical diagnoses.

Statistical analysis

The relationships between demographic variables and clinical status (i.e. diagnosis) were evaluated with Chi-square, ANOVA and Student's *t*-test (Table 1).

Regional values of both cortical diffusion metrics and cortical thickness from the 68 region parcels of the Desikan–Killiany–Tourville atlas were averaged across hemispheres leading to 34 regions of interest that were used in the analyses.

Cortical diffusion and cortical thickness differences across groups

Multiple linear regression models were employed to investigate the differences in cortical diffusion metric and cortical thickness across groups in each region of interest. All models included age and sex as covariates (e.g. $MSD_{ROI} \sim biomarker\text{-}defined\ groups + Age + Sex$; $CT_{ROI} \sim biomarker\text{-}defined\ groups + Age + Sex$; MSD_{ROI} and CT_{ROI} = regional MSD or CT values extracted from a specific region of interest). Statistical significance was set at the False Discovery Rate (FDR) threshold of 0.05, employing the Benjamini–Hochberg procedure. A supplementary analysis using cortical mean diffusivity form the diffusion tensor model was also performed (see Supplementary material). For comparative purposes, the same models were run using regional Aβ- or tau-PET uptake as dependent variables.

Association between cortical diffusion and both Aβ- and tau-PET uptake

Possible associations between regional cortical diffusion and both Aβ- and tau-PET uptake were investigated by multiple linear regression. Aβ- or tau-PET were modelled as dependent variables and age and sex were included as covariates. In regions where this regression revealed a significant association between cortical diffusion and PET uptake, two further analyses were performed. The first, further including tau-PET uptake as covariate, when investigating the association with Aβ or Aβ-PET when investigating the association with tau. A second, including regional cortical thickness in the model as an additional covariate (e.g. main model for Aβ: $A\beta\text{-}PET_{ROI} \sim MSD_{ROI} + Age + Sex$; first subanalysis: $A\beta\text{-}PET_{ROI} \sim MSD_{ROI} + tau\text{-}PET_{ROI} + Age + Sex$; second subanalysis: $A\beta\text{-}PET_{ROI} \sim MSD_{ROI} + CT_{ROI} + Age + Sex$; main model for tau: $tau\text{-}PET_{ROI} \sim MSD_{ROI} + Age + Sex$; first subanalysis: $tau\text{-}PET_{ROI} \sim MSD_{ROI} + A\beta\text{-}PET_{ROI} + Age + Sex$; second subanalysis: $tau\text{-}PET_{ROI} \sim MSD_{ROI} + CT_{ROI} + Age + Sex$; Aβ-, $tau\text{-}PET_{ROI}$ = PET uptake extracted from a specific region of interest). A further sensitivity analysis including both cortical thickness and tau-PET uptake when investigating the association with Aβ or Aβ-PET when investigating the association with tau is included in the Supplementary material (see Supplementary Fig. 1).

The association between cortical diffusion or cortical thickness and both Aβ- and tau-PET uptake was also investigated focusing on two meta-regions of interest, an early-Aβ meta-region of interest and a temporal meta-region of interest. To this end, cortical diffusion metrics, cortical thickness and Aβ-PET uptake were averaged across regions in which Aβ tends to accumulate early in the disease process[41,42] (bilateral insula, precuneus, posterior cingulate, isthmus cingulate, lateral and medial orbitofrontal). Cortical diffusion metrics, cortical thickness and tau-PET uptake were also averaged across temporal regions covering neocortical regions that correspond to Braak staging I to IV.[43] All the meta-regions of interest were weighted by surface areas. Aβ-PET uptake in the early-Aβ meta-region of interest or tau-PET uptake in the temporal meta-region of interest was modelled as the dependent variable in a multiple linear regression, while cortical diffusion metrics or cortical thickness from the same meta-region of interest were used as the independent variable. All models included age and sex as covariates (e.g. $A\beta\text{-}PET_{early\text{-}A\beta} \sim MSD_{early\text{-}A\beta} + Age + Sex$; $A\beta\text{-}PET_{early\text{-}A\beta}$ and $MSD_{early\text{-}A\beta}$ = Aβ-PET and MSD values extracted from the early-Aβ meta-region of interest; $tau\text{-}PET_{temporal} \sim MSD_{temporal} + Age + Sex$; $tau\text{-}PET_{temporal}$ and $MSD_{temporal}$ = tau-PET and MSD values extracted from the temporal meta-region of interest). The strength of the associations between PET uptake (Aβ or tau) and cortical diffusion or cortical thickness were compared by bootstrapping (1000 bootstraps) the standardized beta coefficients from the regression models and comparing the confidence intervals as previously reported.[44] A further analysis restricting the cohort to Aβ-positive participants is reported in the Supplementary Material (see Supplementary material and Supplementary Fig. 2).

Association between cortical diffusion and plasma markers

The association between regional cortical diffusion and both GFAP and NfL was tested in each region of interest in a subset of participants with available an plasma sample (n = 292; 158 Aβ-negative/tau-negative, 90 Aβ-positive/tau-negative and 41 Aβ-positive/tau-positive). In regions where the analysis revealed a significant association, a follow-up analysis including cortical thickness in the model was performed. All models included age and sex as covariates and statistical significance was set to the FDR threshold of 0.05, employing the Benjamini–Hochberg procedure (e.g. main model for GFAP: $GFAP \sim MSD_{ROI} + Age + Sex$; subanalysis: $GFAP \sim MSD_{ROI} + CT_{ROI} + Age + Sex$; main model for NfL: $NfL \sim MSD_{ROI} + Age +$

Sex; subanalysis: $NfL \sim MSD_{ROI} + CT_{ROI} + Age + Sex$). We also investigated the potential mediation effect of GFAP on the association between Aβ-PET and cortical diffusion focusing on the early-Aβ meta-region of interest. To this end we performed a model-based causal mediation analysis based on linear models testing the possible mediation effect using the 'mediate' function, from the R package *mediation*. The statistical significance of the mediation effect was estimated with bootstrapping (10 000 samples).[45]

Association between cortical diffusion and cognitive performance

The clinical relevance of cortical diffusion metrics was further tested by investigating the associations of these metrics with executive and memory functions. The analysis focused on the early-Aβ meta-region of interest and the performance in the trail making test for testing the association with executive function. Recent evidence from our group showed that the difference between the score in the trail making B and the score in the trail making A (trail making B – trail making A) was particularly sensitive to early Aβ pathology.[20] To investigate the association with memory function we focused on the temporal meta-region of interest and on the performance on the Alzheimer's Disease Assessment Scale (ADAS) delayed recall score. Multiple regression models were run on the entire cohort including age, sex and years of education as covariates (e.g. TMT-BA $\sim MSD_{early\text{-}A\beta} + Age + Sex + years\ of\ education$; TMT-BA = trail making B—trail making A; ADAS-delayed $\sim MSD_{temporal} + Age + Sex + years\ of\ education$; ADAS-delayed = ADAS delayed recall score). The strength of the associations between cognitive scores and cortical diffusion or cortical thickness was compared by bootstrapping the standardized beta coefficients as explained above. All analyses were performed in Python 3.7.6 and R v3.6.1.

Data availability

Anonymized data will be shared by request from a qualified academic investigator for the sole purpose of replicating procedures and results presented in the article and as long as data transfer is in agreement with EU legislation on the general data protection regulation and decisions by the Swedish Ethical Review Authority and Region Skåne, which should be regulated in a material transfer agreement.

Results

Regional cortical diffusion differs between biomarker-defined groups

We first focus on the differences in cortical diffusion metrics and cortical thickness between participants stratified based on evidence of Aβ and tau accumulation.

Differences between 'Aβ-negative/tau-negative' and 'Aβ-positive/tau-negative' individuals

MSD revealed widespread microstructural differences, namely higher MSD values in the Aβ-positive/tau-negative group when compared with the Aβ-negative/tau-negative, with a spatial distribution that closely resembled the pattern of Aβ accumulation, including retrosplenial regions extending to the precuneus, neocortical temporal regions, as well as rostral anterior cingulate and rostral middle frontal cortex [standardized-β coefficients range: 0.18 to 0.30; see Fig. 1A(i and iii)] for the corresponding pattern of Aβ-PET uptake). In contrast, differences in cortical thickness were more limited: lower cortical thickness estimates in entorhinal cortex, parahippocampal gyrus and temporal pole for the Aβ-positive/tau-negative group when compared with the Aβ-negative/tau-negative; standardized-β coefficients range: –0.27 to –0.31; Fig. 1A(ii). There was no statistically significant difference in RTOP between the two groups.

Differences between 'Aβ-positive/tau-negative' and 'Aβ-positive/tau-positive' individuals

Difference in MSD between the two groups were widespread, with higher MSD values in the Aβ-positive/tau-positive group, and encompassed both the medial and the lateral portion of the temporal and of the parietal lobe as well as the frontal regions [see Fig. 1B(i); standardized-β coefficients range: 0.30 to 0.74 and Fig. 1B(iv) for the corresponding pattern of differences in tau-PET uptake]. Difference in cortical thickness between the two group were more limited with significantly lower estimates of cortical thickness for the Aβ-positive/tau-positive group in specific regions of the temporal and parietal lobe [see Fig. 1B(ii); standardized-β coefficients range: –0.42 to –0.73]. There was no statistically significant difference in RTOP between the two groups.

Regional cortical diffusion is associated with Aβ–PET uptake independently of tau and cortical thinning

Considering the clear differences in cortical diffusion captured by MSD, we aimed to study its biological underpinnings. Parallel analysis employing RTOP have been also performed and are presented in the Supplementary material and Supplementary Fig. 3. The regression analysis showed widespread positive associations between regional MSD and regional Aβ-PET uptake in the full cohort, with higher standardized-β values in lateral–temporal and retrosplenial regions [Fig. 2A(i); standardized-β coefficients range: 0.12–0.38]. When including tau-PET uptake from the same region in the regression analysis, the results remained substantially unchanged except for the medial temporal regions in which the association between MSD and Aβ-PET was no longer significant [Fig. 2A(ii); standardized-β coefficients range: 0.11–0.20]. Another sensitivity analysis including regional cortical thickness revealed consistent results, especially in lateral temporal regions as well as in medial parietal and frontal regions, although less widespread [Fig. 2A(iii); standardized-β coefficients range: 0.13–0.34].

The analysis focusing on the early-Aβ meta-region of interest provided converging evidence showing that MSD was associated with Aβ-PET uptake (MSD: standardized-$\beta = 0.33$, $P < 0.001$; Fig. 3A and Supplementary Table 1). Cortical thickness was also associated with Aβ-PET uptake in the same meta-region of interest (cortical thickness: standardized-$\beta = -0.18$, $P < 0.001$; Fig. 3B and Supplementary Table 2). However, there was a significant difference between the β coefficients of MSD and cortical thickness ($P < 0.01$), revealing that the association to Aβ-PET uptake was stronger for MSD than for cortical thickness. The supplementary analysis restricted to Aβ-positive participants led to consistent results showing a significant association between MSD and Aβ-PET uptake (MSD: standardized-$\beta = 0.14$, $P < 0.05$) but no association between cortical thickness and Aβ-PET uptake (cortical thickness: standardized-$\beta = -0.06$, $P > 0.3$; see Supplementary material, Supplementary Fig. 2 and Supplementary Tables 9 and 10).

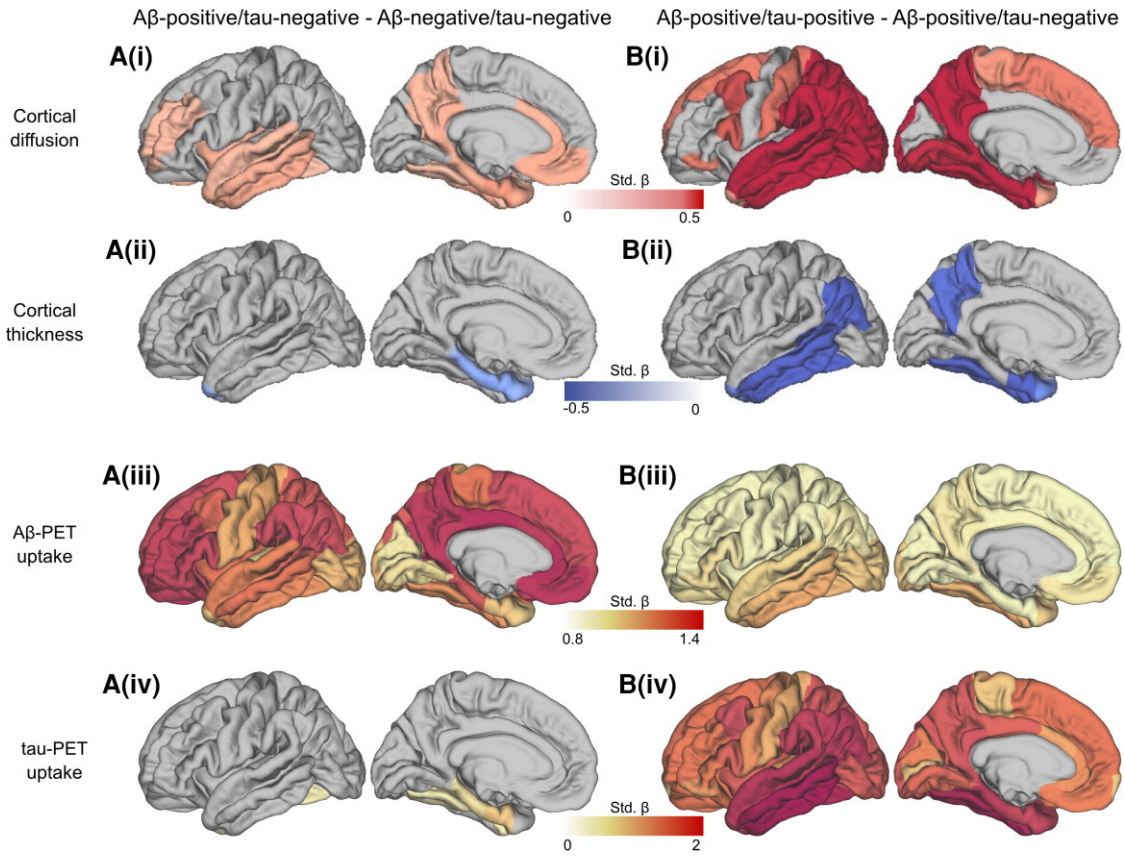

Figure 1 Regional cortical diffusion and cortical thickness differences across groups. The colour scale represents standardized β values from the multiple regression model comparing the metric of interest (cortical diffusion or cortical thickness) across groups. For visualization purposes the standardized β values of each region of interest have been plotted on a standard cortical surface. Only results corrected for multiple comparisons are displayed (FDR, $P < 0.05$). The differences across groups in both Aβ-PET uptake [**A(iii)** and **B(iii)**] and tau-PET uptake [**A(iv)** and **B(iv)**] have been included for comparative purposes. [**A(i)**] Difference in cortical diffusion (mean squared displacement, MSD) between Aβ-negative/tau-negative and Aβ-positive/tau-negative participants. [**A(ii)**] Difference in cortical thickness between Aβ-negative/tau-negative and Aβ-positive/tau-negative participants. [**A(iii)**] Difference in Aβ-PET uptake between Aβ-negative/tau-negative and Aβ-positive/tau-negative participants. [**A(iv)**] Difference in tau-PET uptake between Aβ-negative/tau-negative and Aβ-positive/tau-negative participants. [**B(i)**] Difference in cortical diffusion (mean squared displacement) between Aβ-positive/tau-negative and Aβ-positive/tau-positive participants. [**B(ii)**] Difference in cortical thickness between Aβ-positive/tau-negative and Aβ-positive/tau-positive participants. [**B(iii)**] Difference in Aβ-PET uptake between Aβ-positive/tau-negative and Aβ-positive/tau-positive participants. [**B(iv)**] Difference in tau-PET uptake between Aβ-positive/tau-negative and Aβ-positive/tau-positive participants.

Regional cortical diffusion is associated with tau-PET uptake independently of Aβ and cortical thinning

Regional MSD was also positively associated with regional tau-PET uptake with a spatial pattern that closely resembled the stereotypical distribution of tau accumulation [Fig. 2B(i); standardized-β coefficients range: 0.15–0.53]. When including Aβ-PET uptake in the model the pattern of positive associations between MSD and tau-PET remained consistent with the results of the previous analysis [Fig. 2B(ii); standardized-β coefficients range: 0.11–0.40]. Virtually the same pattern of results held when accounting for regional cortical thickness in the models [Fig. 2B(iii); standardized-β coefficients range: 0.14–0.47] showing that the regional association between MSD and tau-PET uptake was independent from Aβ-PET uptake and cortical thickness.

The analysis focusing on the temporal meta-region of interest provided similar results showing that MSD was associated with tau-PET uptake (MSD: standardized-$\beta = 0.48$, $P < 0.001$; Fig. 3C and Supplementary Table 3). Cortical thickness was also associated with tau-PET uptake (cortical thickness: standardized-$\beta = -0.35$, $P < 0.001$; Fig. 3C and Supplementary Table 4). However, tau-PET uptake was more strongly associated with MSD than with cortical thickness, as the magnitude of the standardized-β coefficients were significantly lower for cortical thickness than for MSD ($P < 0.01$). The supplementary analysis restricted to Aβ-positive participants led to consistent results showing a significant association between both MSD and cortical thickness and tau-PET uptake (MSD: standardized-$\beta = 0.53$, $P < 0.001$; cortical thickness: standardized-$\beta = -0.45$, $P < 0.001$). In this case the associations had a similar magnitude (see Supplementary material, Supplementary Fig. 1 and Supplementary Tables 11 and 12).

Plasma levels of GFAP are associated with regional cortical diffusion and partially mediated the effect of Aβ-PET on cortical diffusion

In the subgroup of participants with available plasma GFAP ($n = 292$), regional MSD was positively associated with GFAP with a pattern that resembles Aβ accumulation (Fig. 4A; standardized-β coefficients range: 0.14–0.20). Even when including cortical thickness in the model such association remained

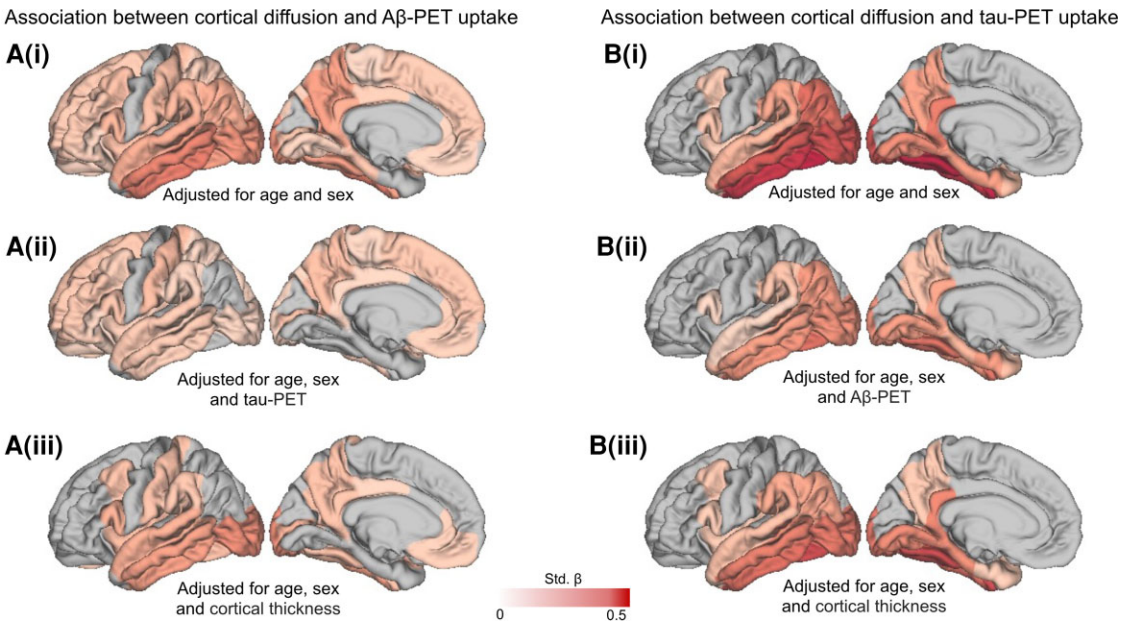

Figure 2 Association between cortical diffusion and both Aβ- and tau-PET uptake across neocortical regions. The colour scale represents standardized β values from the multiple regression model testing the association between cortical diffusion (mean squared displacement; MSD) and Aβ-PET uptake [**A(i–iii)**] or tau-PET uptake [**B(i–iii)**]. For visualization purposes the standardized β values of each region of interest have been plotted on a standard cortical surface. Only results corrected for multiple comparisons are displayed (FDR, $P < 0.05$). [**A(i)**] Regional association between MSD and Aβ-PET uptake. [**A(ii)**] Regional association between MSD and Aβ-PET uptake including tau-PET uptake from the same region as a covariate in the model. [**A(iii)**] Regional association between MSD and Aβ-PET uptake including mean cortical thickness of the same region as a covariate in the model. [**B(i)**] Regional association between MSD and tau-PET uptake. [**B(ii)**] Regional association between MSD and tau-PET uptake including Aβ-PET uptake from the same region as a covariate in the model. [**B(iii)**] Regional association between MSD and tau-PET uptake including mean cortical thickness of the same region as a covariate in the model.

statistically significant in several temporal, parietal and frontal regions (Fig. 4B; standardized-β coefficients range: 0.15–0.23). Considering the well-known association between astrocytic activation and Aβ pathology and the positive association between cortical diffusion and both Aβ and GFAP, we conducted a mediation analysis between these variables focusing on the early-Aβ meta-region of interest. The results revealed that GFAP partially mediated the association between Aβ-PET uptake in a composite neocortical region and MSD from the same region (standardized-β = 0.026, 95% CI = 0.060–0.038, $P < 0.05$, mediated effect = 15%; Fig. 4B and C).

Plasma levels of NfL are associated with regional cortical diffusion

In the subgroup of participants with available plasma samples ($n = 292$), regional MSD was positively associated with NfL in several neocortical regions (Fig. 5A; standardized-β coefficients range: 0.14–0.29). Including cortical thickness in the model essentially did not affect the pattern of associations between NfL and MSD (Fig. 4B; standardized-β coefficients range: 0.14–0.34). The positive association between NfL and MSD was also confirmed when extracting the MSD values from both the early-Aβ and the temporal meta-regions of interest (early-Aβ meta-region of interest: standardized-β = 0.20, $P < 0.01$; early-Aβ meta-region of interest: standardized-β = 0.26, $P < 0.001$; see Fig. 5C and D). Moreover, such association between NfL and MSD was significantly stronger than the association between NfL levels and cortical thickness extracted from the same meta-regions of interest (both *P*-values <0.05).

Regional cortical diffusion is associated with cognitive deficit

In the early-Aβ meta-region of interest, MSD was associated with performance in the trail making test (trail making B – trail making A), which reflects executive functions and has been previously related to early Aβ pathology[20] (standardized-β = 0.33, $P < 0.001$; see Fig. 6A and Supplementary Table 5). Cortical thickness was also associated executive functions (standard-β = –0.15, $P < 0.01$; see Fig. 6B and Supplementary Table 6), but the comparison between standardized β-coefficients showed that the association between MSD and executive functions was stronger than the association between cortical thickness and executive functions ($P < 0.001$). Likewise, MSD in the temporal meta-region of interest was associated with the ADAS delayed recall score (standardized-β = 0.38, $P < 0.001$; see Fig. 6C and Supplementary Table 7). A similar relationship was found between cortical thickness and ADAS delayed recall (standardized-β = –0.24, $P < 0.001$; see Fig. 6D and Supplementary Table 8), but the standardized β-coefficients differed such that MSD was more strongly associated than cortical thickness to ADAS delayed recall score ($P < 0.001$).

Supplementary sensitivity analyses

We also performed three main supplementary sensitivity analyses to further test our hypotheses. First, the main analyses involving cortical diffusion metrics were repeated including *APOE* status as a covariate in the models (coded as a binary value, i.e. ϵ4 carriers and non ϵ4 carriers). The inclusion of *APOE* did not affect either the differences in cortical diffusion between groups or the associations between cortical diffusion and other markers of the Alzheimer's disease pathological cascade (see Supplementary Fig. 4). Second, supplementary analyses

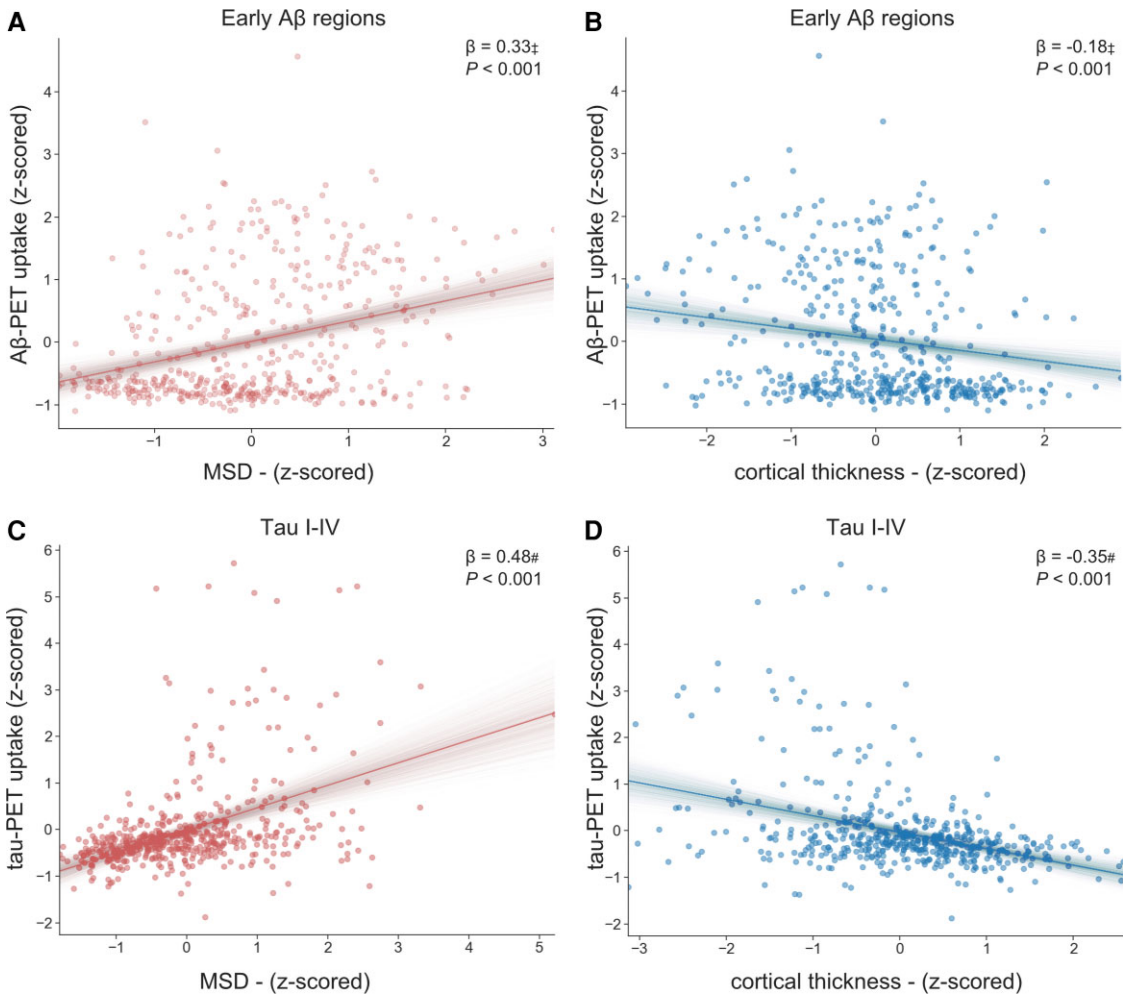

Figure 3 Association between cortical diffusion and cortical thickness with both Aβ- and tau-PET uptake in selected meta-regions of interest. Associations between cortical diffusion (mean squared displacement; MSD) and cortical thickness with Aβ- or tau-PET in two meta-regions of interest, namely an early-Aβ meta-region of interest and a temporal neocortical meta-region of interest. β and P: standardized β coefficients and P-values for the association of interest from multiple regression model, which included age and sex as covariates (as described in the main text). ‡Statistically significant difference between the standardized β coefficients of MSD and cortical thickness on Aβ-PET uptake. #Statistically significant difference between the standardized β coefficients of MSD and cortical thickness on tau-PET uptake. (**A**) Association between cortical diffusion and Aβ-PET uptake in a meta-region of interest encompassing regions that accumulate Aβ early in the disease process. (**B**) Association between cortical thickness and Aβ-PET uptake in the early-Aβ meta-region of interest. (**C**) Association between cortical diffusion and tau-PET uptake in a temporal meta-regions of interest including cortical regions approximating Braak stages I–IV. (**D**) Association between cortical thickness and tau-PET uptake in the temporal meta-region of interest. The translucent area around the regression lines represents the 95% confidential interval for the regression estimate.

focusing on participants older than 65 years were performed to ensure the main results were applicable to late-onset Alzheimer's disease. Also in this case, the supplementary analysis confirmed the main results (see Supplementary Tables 13–18). Third, the comparison between biomarker-defined groups as well as the investigation of the association between cortical diffusion and both Aβ- and tau-PET uptake were repeated using mean diffusivity (MD) from the diffusion tensor model. The results were very consistent with the results obtained employing MSD although both Aβ- and tau-PET uptake were more strongly associated with MSD than with MD, as the magnitude of the standardized β coefficients were significantly lower for MD than for MSD ($P < 0.05$; see Supplementary material and Supplementary Fig. 5).

Discussion

In an era of clinical trials of disease-modifying therapies that move toward the early phases of the Alzheimer's disease pathological cascade, there is an urgent need to develop markers that can trace even subtle events downstream from protein accumulation as well as response to treatments. Standard morphological metrics such as regional cortical thickness or hippocampal volume might not be well equipped to meet this challenge considering that they are mainly sensitive to atrophy. Microstructural changes can occur before overt atrophy becomes visible and there is an increasing interest in employing dMRI to detect such changes in affected cortical regions.[11,13,14,18,46] The current study provided clear evidence of the sensitivity of cortical diffusion and, specifically, mean squared displacement from MAP-MRI, to pathological changes related to both Aβ and tau pathology in a large cohort of participants from the Swedish BioFINDER-2 study.

MSD revealed widespread microstructural differences already between 'Aβ-negative/tau-negative' and 'Aβ-positive/tau-negative' participants with a spatial distribution that closely resembled the pattern of Aβ accumulation. In contrast, differences in cortical

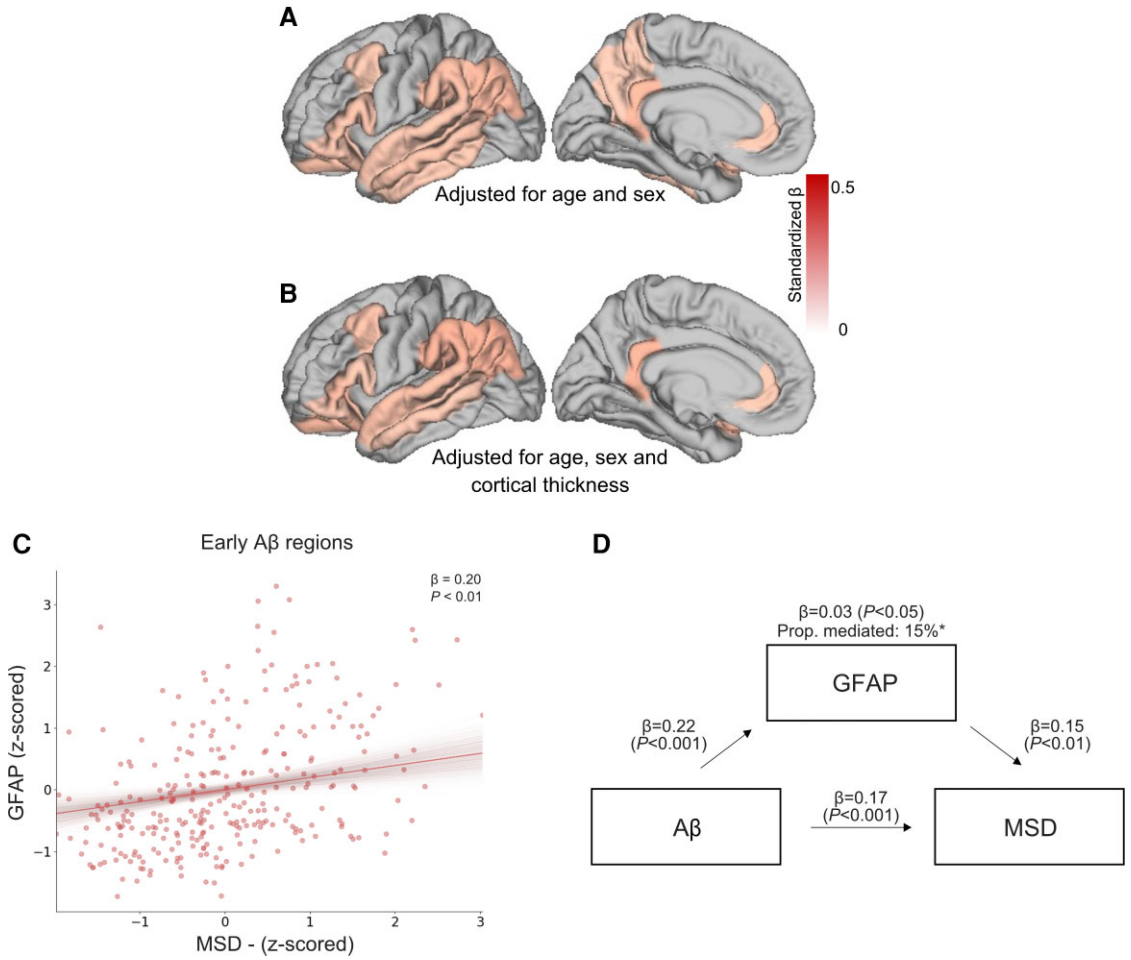

Figure 4 Association between cortical diffusion and plasma level of GFAP. (**A**) Regional associations between cortical diffusion (MSD) and plasma level of GFAP. (**B**) Regional associations between MSD and GFAP including mean cortical thickness from the same region as a covariate in the model. The colour scale represents standardized β values from the multiple regression model. For visualization purposes the standardized β values of each region of interest have been plotted on a standard cortical surface. Only results corrected for multiple comparisons are displayed (FDR, $P < 0.05$). (**C**) association between MSD and GFAP in the early-Aβ meta-region of interest (standardized-β = 0.20, $P < 0.01$). The translucent area around the regression line represents the 95% confidential interval for the regression estimate. (**D**) Flow chart representing the partial mediation effect of GFAP on the association between Aβ-PET uptake and MSD in the early-Aβ meta-region of interest.

thickness were clearly more limited. MSD was also highly correlated with both Aβ- and tau-PET uptake even independently from one another as well as independently from cortical thickness. The analysis focusing on a meta-region of interest reflecting the regions sensitive to Aβ accumulation early in the disease stage confirmed that MSD was more sensitive than cortical thickness to Aβ-related pathological processes. When investigating the association with tau-PET uptake in a temporal meta-region of interest a similar result was found. Increased MSD also correlated significantly better than cortical thickness with both executive and memory functions, providing further evidence that differences in cortical diffusion are of clinical relevance. Moreover, regional MSD values were associated with plasma level of GFAP with a pattern that resembles Aβ accumulation, and GFAP partially mediated the association between Aβ and MSD, pointing to a link between an increase in cortical diffusivity and astrogliosis.

Cortical diffusivity was more sensitive than cortical thickness across the entire the spectrum of analysis we performed even when looking at the association with another marker of neurodegeneration such as plasma levels of NfL. MSD is a metric that captures the average amount of diffusivity in the tissue, thus multiple physiological processes can contribute to changes in such a metric. The lack of biological specificity could pose a limitation especially when compared with a metric from biophysical modelling that tries to disentangle different tissue components from one another (e.g. neurites from free water). However, the interpretation of dMRI metrics using biophysical models comes at the cost of theoretical assumption. Different but seemingly acceptable assumptions lead to conflicting directions of change when comparing, for example, brain regions.[28,29] In our study, we provide evidence of the biological substrate leading to difference in cortical diffusion by leveraging the multimodal design. In line with a recent reports based on mean diffusivity from DTI,[14] we showed that the increase in cortical diffusion was associated with tau-PET uptake with a spatial distribution that follows the stereotypical spread of tau pathology in late-onset Alzheimer's disease. However, here we also reported a clear association with Aβ-PET uptake, which, to our knowledge, has not been reported so far, which has clear implications for anti-Aβ trials.

In the context of the investigation of early markers of downstream events for clinical trials, the association between cortical

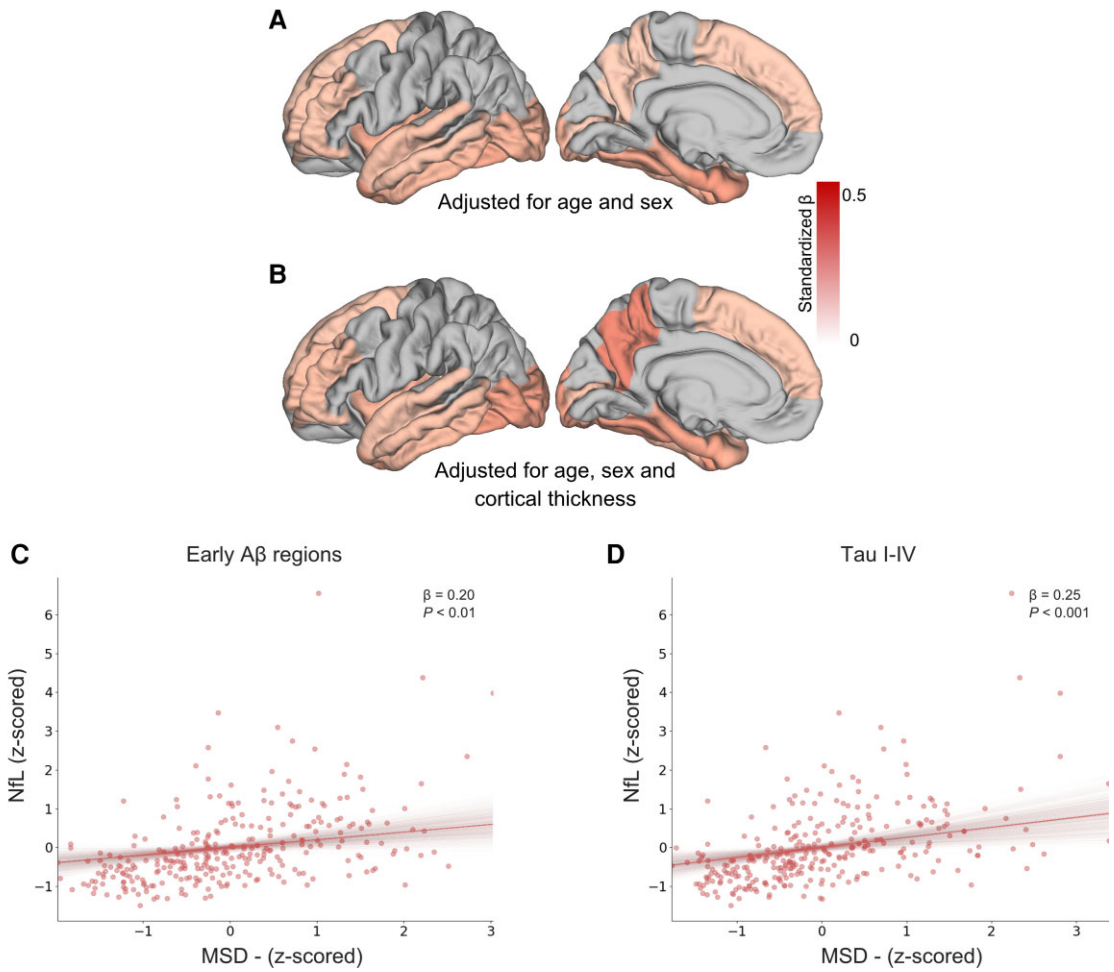

Figure 5 Association between cortical diffusion and plasma level of NfL. (**A**) Regional associations between cortical diffusion (MSD) and plasma level of NfL. (**B**) Regional associations between MSD and NfL including mean cortical thickness from the same region as a covariate in the model. The colour scale represents standardized β values from the multiple regression model. For visualization purposes the standardized β values of each region of interest have been plotted on a standard cortical surface. Only results corrected for multiple comparisons are displayed (FDR, $P < 0.05$). (**C**) Association between MSD and NfL in the early-Aβ meta-region of interest (standardized-$\beta = 0.20$, $P < 0.01$). (**D**) Association between MSD and NfL in the temporal meta-region of interest (standardized-$\beta = 0.25$, $P < 0.001$). The translucent area around the regression line represents the 95% confidential interval for the regression estimate.

diffusion and Aβ-PET uptake is particularly relevant. Differences in cortical diffusion were already detectable between 'Aβ-negative/tau-negative' and 'Aβ-positive/tau-negative' and an increase in Aβ-PET uptake was associated with an increase in MSD independently of tau accumulation. MSD in the early-Aβ meta-region of interest was also associated with performance in executive function, which is in agreement with a recent study showing that the used executive task is one of the most sensitive cognitive tests to early Aβ pathology.[20] This converging evidence suggested cortical diffusion could be an early putative marker of pathological events downstream from Aβ accumulation. Only one study has previously investigated the association between Aβ-PET uptake and metrics of cortical diffusion, but it found no significant result.[14] However, the work included only healthy elderlies and the proportion of Aβ positive individuals, according to their PET uptake cut-off, was lower compared to the present study (49 Aβ-positive individuals compared to 147 Aβ-positive/tau-negative individuals in our study).

A further interesting result of this study is the association between cortical diffusion and plasma level of the glial marker GFAP, which appear to be largely independent from cortical thickness. Neuroinflammation, including astrocytic activation and astrocytosis, accompanies Aβ accumulation[22,47] and astrocytes are likely to participate in Aβ clearance.[48,49] Reactive astrocytes are characterized by an increased production of GFAP and hypertrophy,[22,50] which could modify the microstructural environment of the affected cortical regions. Such difference would likely alter water diffusivity becoming detectable by dMRI. Furthermore, immunotherapies directed against Aβ are likely to modify the neuroinflammatory response as a secondary effect to the reduction of Aβ-plaques.[8] This change could also modify the microstructural environment and, potentially, be captured by dMRI. The link between Aβ accumulation, astrocytosis and cortical diffusion is further supported by the results of the mediation analysis, revealing a mediation effect of GFAP on the association between Aβ and cortical diffusion. Although the proportion of effect mediated by GFAP is limited (15%), these results suggest a cortical diffusion is partially sensitive to pathological events other than neurodegeneration.

Some limitation should be considered when interpreting the results of the study. Diffusion MRI data are typically acquired with a resolution that is much coarser than the resolution of anatomical

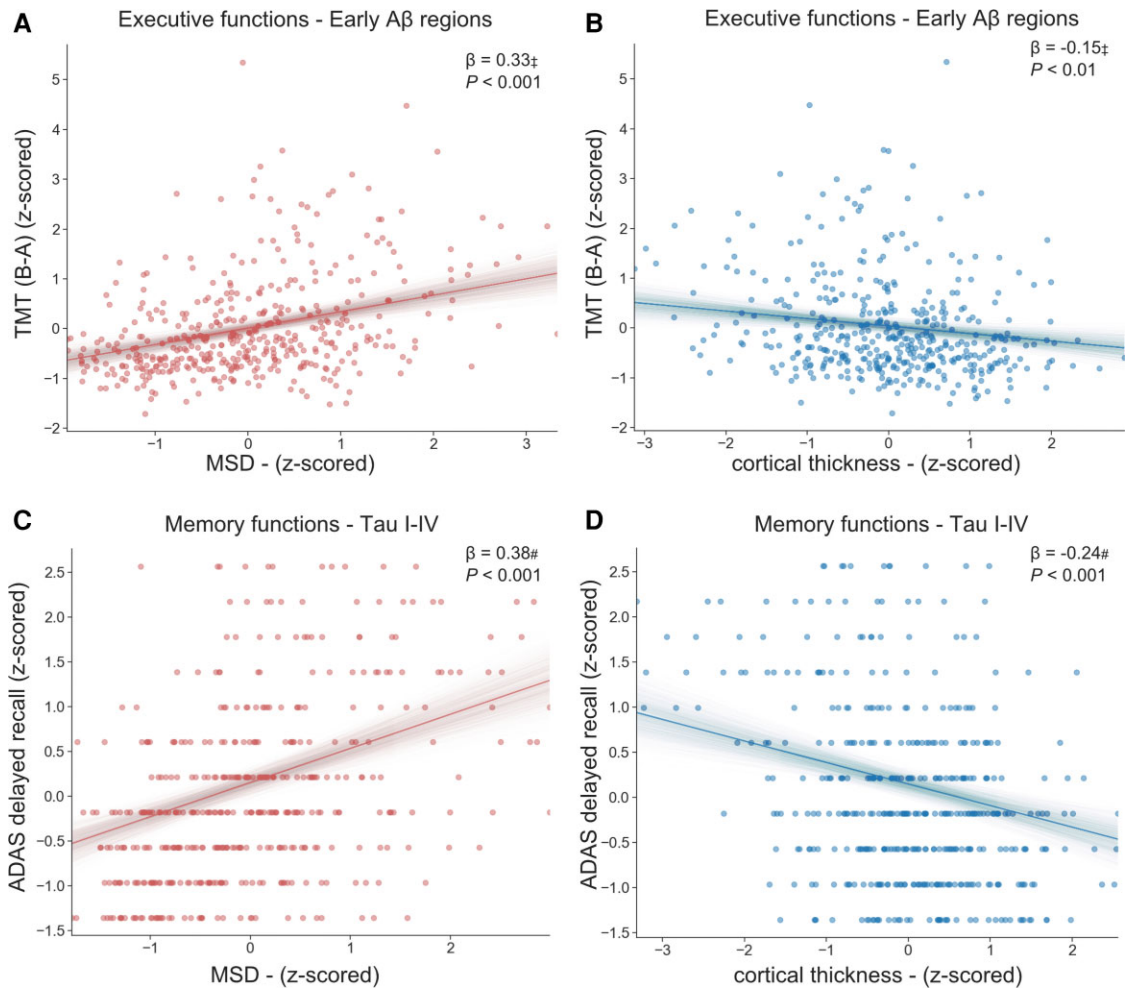

Figure 6 Association between cortical diffusion and cognitive performance. Associations between cortical diffusion (mean squared displacement; MSD) and cortical thickness with measures of executive and memory functions. β and P: standardized β coefficients and P-values for the association of interest from a multiple regression model, which included age and sex as covariates (as described in the main text). ‡Statistically significant difference between the standardized β coefficients of MSD and cortical thickness on the TMT score (trail-B – trail-A; measure of executive functions). #Statistically significant difference between the standardized β coefficients of MSD and cortical thickness on ADAS delayed recall score (measure of memory functions). (**A**) Association between MSD and TMT (trail making B – trail making A) in the early-Aβ meta-region of interest. (**B**) Association between cortical thickness and TMT (trail making B – trail making A) in the early-Aβ meta-region of interest. (**C**) Association between MSD and ADAS delayed recall score in the temporal meta-region of interest. (**D**) Association between cortical thickness and ADAS delayed recall score in the temporal meta-region of interest. The translucent area around the regression lines represents the 95% confidential interval for the regression estimate.

images (e.g. $2 \times 2 \times 2$ mm^3). Considering the thickness of the cortical ribbon varies between 1.5 and 4 mm depending on the brain region, metrics extracted from cortical regions of interest are going to be contaminated by partial volume effects. We applied a state-of-the-art processing pipeline to alleviate this problem that, nevertheless, remains one of the main limitations of our study as well as of other studies in this field employing clinically available diffusion MRI protocols. Another limitation is the cross-sectional nature of the study. We discussed the possible role of metric of cortical diffusion as markers in clinical trials, but further work is needed to test the sensitivity of the metrics in a longitudinal design. In addition, we focused on MSD because MAP-MRI allowed us to take full advantage the diffusion MRI data we were employing. However, further research is needed to clarify which metric derived from diffusion MRI would be the best surrogate marker of cortical microstructural changes related to the Alzheimer's disease pathological cascade. Both advantages and generalizability of results obtained with different analysis approaches, including diffusion tensor imaging and multicompartment models like the SANDI[51] or NODDI, should be directly compared on the same cohorts. For example, our supplementary analysis using mean diffusivity (MD) from the diffusion tensor model showed that MD performed very similarly to MSD, although both Aβ- and tau-PET uptake were more strongly associated with MSD than with MD (see Supplementary material). Another limitation of the study is the lack of plasma sample for some participants. However, the subgroup analysis including GFAP and NfL was still performed in a group of 292 participants.

With these limitations in mind, the current results showed that cortical diffusion is highly sensitive to multiple aspects of the pathological cascade of Alzheimer's disease. Of particular interest is the link with both Aβ-PET and GFAP, which suggests cortical diffusion might reflect microstructural changes related to the astrocytic response to Aβ aggregation in addition to subtle neurodegenerative processes. Therefore, cortical diffusion emerges as a potential putative marker to help monitoring the early stage of Alzheimer's disease

process and even more importantly the response to anti-Aβ treatments in clinical trials.

Funding

Work at the authors' research centre was supported by the Swedish Research Council (2016-00906), the Knut and Alice Wallenberg foundation (2017-0383), the Marianne and Marcus Wallenberg foundation (2015-0125), the Strategic Research Area MultiPark (Multidisciplinary Research in Parkinson's disease) at Lund University, the Alzheimerfonden (AF-939932), the Swedish Brain Foundation (FO2021-0293), the Konung Gustaf V:s och Drottning Victorias Frimurarestiftelse, the Skåne University Hospital Foundation (2020-O000028), Regionalt Forskningsstöd (2020-0314) and the Swedish Federal Government under the ALF agreement (2018-Projekt0279). The precursor of ^{18}F-flutemetamol was sponsored by GE Healthcare. The precursor of ^{18}F-RO948 was provided by Roche. The funding sources had no role in the design and conduct of the study; in the collection, analysis, interpretation of the data; or in the preparation, review or approval of the manuscript.

Competing interests

O.H. has acquired research support (for the institution) from ADx, AVID Radiopharmaceuticals, Biogen, Eli Lilly, Eisai, Fujirebio, GE Healthcare, Pfizer and Roche. In the past 2 years, he has received consultancy/speaker fees from Amylyx, Alzpath, BioArctic, Biogen, Cerveau, Fujirebio, Genentech, Novartis, Roche and Siemens.

Supplementary material

Supplementary material is available at *Brain* online.

References

1. Masters CL, Bateman R, Blennow K, Rowe CC, Sperling RA, Cummings JL. Alzheimer's disease. *Nat Rev Dis Primers*. 2015;1:15056.
2. Hansson O. Biomarkers for neurodegenerative diseases. *Nat Med*. 2021;27:954-963.
3. Cullen NC, Zetterberg H, Insel PS, *et al*. Comparing progression biomarkers in clinical trials of early Alzheimer's disease. *Ann Clin Transl Neurol*. 2020;7:1661-1673.
4. Mintun MA, Lo AC, Duggan Evans C, *et al*. Donanemab in early Alzheimer's disease. *N Eng J Med*. 2021;384:1691-1704.
5. Swanson CJ, Zhang Y, Dhadda S, *et al*. A randomized, double-blind, phase 2b proof-of-concept clinical trial in early Alzheimer's disease with lecanemab, an anti-aβ protofibril antibody. *Alzheimer's Res Ther*. 2021;13:1-14.
6. Salloway S, Farlow M, McDade E, *et al*. A trial of gantenerumab or solanezumab in dominantly inherited Alzheimer's disease. *Nat Med*. 2021;27:1187-1196.
7. Salloway S, Sperling R, Fox NC, *et al*. Two phase 3 trials of bapineuzumab in mild-to-moderate Alzheimer's disease. *N Eng J Med*. 2014;370:322-333.
8. Zotova E, Bharambe V, Cheaveau M, *et al*. Inflammatory components in human Alzheimer's disease and after active amyloid-β42 immunization. *Brain*. 2013;136:2677-2696.
9. Novak G, Fox N, Clegg S, *et al*. Changes in brain volume with bapineuzumab in mild to moderate Alzheimer's disease. *J Alzheimer's Dis*. 2016;49:1123-1134.
10. Le Bihan D, Breton E. Imagerie de diffusion in-vivo par résonance magnétique nucléaire. *Comptes-Rendus de l'Académie des Sciences*. 1985;93:27-34.
11. Illán-Gala I, Montal V, Borrego-Écija S, *et al*. Cortical microstructure in the behavioural variant of frontotemporal dementia: Looking beyond atrophy. *Brain*. 2019;142:1121-1133.
12. Vilaplana E, Rodriguez-Vieitez E, Ferreira D, *et al*. Cortical microstructural correlates of astrocytosis in autosomal-dominant Alzheimer disease. *Neurology*. 2020;94:e2026-e2036.
13. Montal V, Vilaplana E, Alcolea D, *et al*. Cortical microstructural changes along the Alzheimer's disease continuum. *Alzheimer's Dement*. 2018;14:340-351.
14. Rodriguez-Vieitez E, Montal V, Sepulcre J, *et al*. Association of cortical microstructure with amyloid-β and tau: Impact on cognitive decline, neurodegeneration, and clinical progression in older adults. *Mol Psychiatry*. 2021;26:1-10.
15. Zhang H, Schneider T, Wheeler-Kingshott CA, Alexander DC. NODDI: Practical *in vivo* neurite orientation dispersion and density imaging of the human brain. *Neuroimage*. 2012;61:1000-1016.
16. Gozdas E, Fingerhut H, Dacorro L, Bruno JL, Hosseini SMH. Neurite imaging reveals widespread alterations in gray and white matter neurite morphology in healthy aging and amnestic mild cognitive impairment. *Cereb Cortex*. 2021;31:5570-5578.
17. Vogt NM, Hunt JF, Adluru N, *et al*. Cortical microstructural alterations in mild cognitive impairment and Alzheimer's disease dementia. *Cereb Cortex*. 2020;30:2948-2960.
18. Vogt NM, Hunt JFV, Adluru N, *et al*. Interaction of amyloid and tau on cortical microstructure in cognitively unimpaired adults. *Alzheimer's Dement*. 2022;18:65-76.
19. Jack CR, Bennett DA, Blennow K, *et al*. NIA-AA Research framework: Toward a biological definition of Alzheimer's disease. *Alzheimer's Dement*. 2018;14:535-562.
20. Tideman P, Stomrud E, Leuzy A, Mattsson-Carlgren N, Palmqvist S, Hansson O. Association of β-amyloid accumulation with executive function in adults with unimpaired cognition. *Neurology*. 2022;98:e1525-e1533.
21. Spanos F, Liddelow SA. An overview of astrocyte responses in genetically induced Alzheimer's disease mouse models. *Cells*. 2020;9:1-33.
22. Arranz AM, De Strooper B. The role of astroglia in Alzheimer's disease: Pathophysiology and clinical implications. *Lancet Neurol*. 2019;18:406-414.
23. Zhang K, Programs F, Boe C, *et al*. Complement and microglia mediate early synapse loss in Alzheimer mouse models. *Science*. 2016;352:712-716.
24. Pereira JB, Janelidze S, Smith R, *et al*. Plasma GFAP is an early marker of amyloid-β but not tau pathology in Alzheimer's disease. *Brain*. 2021;144:3505-3516.
25. Özarslan E, Koay CG, Shepherd TM, *et al*. Mean apparent propagator (MAP) MRI: A novel diffusion imaging method for mapping tissue microstructure. *Neuroimage*. 2013;78:16-32.
26. Fick RHJ, Wassermann D, Caruyer E, Deriche R. MAPL: Tissue microstructure estimation using Laplacian-regularized MAP-MRI and its application to HCP data. *Neuroimage*. 2016;134:365-385.
27. Avram AV, Sarlls JE, Barnett AS, *et al*. Clinical feasibility of using mean apparent propagator (MAP) MRI to characterize brain tissue microstructure. *Neuroimage*. 2016;127:422-434.
28. Lampinen B, Szczepankiewicz F, Mårtensson J, van Westen D, Sundgren PC, Nilsson M. Neurite density imaging versus imaging of microscopic anisotropy in diffusion MRI: A model comparison using spherical tensor encoding. *Neuroimage*. 2017;147:517-531.
29. Lampinen B, Szczepankiewicz F, Novén M, *et al*. Searching for the neurite density with diffusion MRI: Challenges for biophysical modeling. *Hum Brain Mapp*. 2019;40:2529-2545.

30. Palmqvist S, Janelidze S, Quiroz YT, *et al*. Discriminative accuracy of plasma phospho-tau217 for Alzheimer disease vs other neurodegenerative disorders. *JAMA*. 2020;324:772-781.
31. Leuzy A, Smith R, Ossenkoppele R, *et al*. Diagnostic performance of RO948 F 18 tau positron emission tomography in the differentiation of Alzheimer disease from other neurodegenerative disorders. *JAMA Neurol*. 2020;77:955-965.
32. Griswold MA, Jakob PM, Heidemann RM, *et al*. Generalized autocalibrating partially parallel acquisitions (GRAPPA). *Magn Reson Med*. 2002;47:1202-1210.
33. Sled JG, Zijdenbos AP, Evans AC. A nonparametric method for automatic correction of intensity nonuniformity in MRI data. *IEEE Trans Med Imaging*. 1998;17:87-97.
34. Ségonne F, Dale AM, Busa E, *et al*. A hybrid approach to the skull stripping problem in MRI. *Neuroimage*. 2004;22:1060-1075.
35. Dale AM, Fischl B, Sereno MI. Cortical surface-based analysis I. Segmentation and surface reconstruction. *Neuroimage*. 1999; 9:179-194.
36. Fischl B, Salat DH, Busa E, *et al*. Whole brain segmentation: Automated labeling of neuroanatomical structures in the human brain. *Neuron*. 2002;33:341-355.
37. Fischl B, Dale AM. Measuring the thickness of the human cerebral cortex. *Proc Natl Acad Sci U S A*. 2000;97:11050-11055.
38. Mitra PP, Latour LL, Kleinberg RL, Sotak CH. Pulsed-field-gradient NMR measurements of restricted diffusion and the return-to-the-origin probability. *J Magn Reson*. 1995;114:47-58.
39. Schwartz LM, Hürlimann MD, Dunn KJ, Mitra PP, Bergman DJ. Restricted diffusion and the return to the origin probability at intermediate and long times. *Phys Rev E*. 1997;55:4225-4234.
40. Menon V, Gallardo G, Pinsk MA, *et al*. Microstructural organization of human insula is linked to its macrofunctional circuitry and predicts cognitive control. *Elife*. 2020;9:1-27.
41. Palmqvist S, Schöll M, Strandberg O, *et al*. Earliest accumulation of β-amyloid occurs within the default-mode network and concurrently affects brain connectivity. *Nat Commun*. 2017;8:1214.
42. Mattsson N, Palmqvist S, Stomrud E, Vogel J, Hansson O. Staging β-amyloid pathology with amyloid positron emission tomography. *JAMA Neurol*. 2019;76:1319-1329.
43. Cho H, Choi JY, Hwang MS, *et al*. In vivo cortical spreading pattern of tau and amyloid in the Alzheimer disease spectrum. *Ann Neurol*. 2016;80:247-258.
44. Janelidze S, Stomrud E, Smith R, *et al*. Cerebrospinal fluid p-tau217 performs better than p-tau181 as a biomarker of Alzheimer's disease. *Nat Commun*. 2020;11:1-12.
45. Hayes AF. Beyond Baron and Kenny: Statistical mediation analysis in the new millennium. *Commun Monogr*. 2009;76:408-420.
46. Broad RJ, Gabel MC, Dowell NG, *et al*. Neurite orientation and dispersion density imaging (NODDI) detects cortical and corticospinal tract degeneration in ALS. *J Neurol Neurosurg Psychiatry*. 2019;90:404-411.
47. Frost GR, Li YM. The role of astrocytes in amyloid production and Alzheimer's disease. *Open Biol*. 2017;7:1-14.
48. Ries M, Sastre M. Mechanisms of aβ clearance and degradation by glial cells. *Front Aging Neurosci*. 2016;8:160.
49. Hou L, Liu Y, Wang X, *et al*. The effects of amyloid-β 42 oligomer on the proliferation and activation of astrocytes in vitro. *In Vitro Cell Dev Biol Anim*. 2011;47:573-580.
50. Rodríguez-Arellano JJ, Parpura V, Zorec R, Verkhratsky A. Astrocytes in physiological aging and Alzheimer's disease. *Neuroscience*. 2016;323:170-182.
51. Palombo M, Ianus A, Guerreri M, *et al*. SANDI: A compartment-based model for non-invasive apparent soma and neurite imaging by diffusion MRI. *Neuroimage*. 2020;215:116835.